Journal of Molecular Structure 1379 (2027) 147346

Contents lists available at ScienceDirect

Journal of Molecular Structure

journal homepage: www.elsevier.com/locate/molstr

Photochemical behavior of novel curcumin-pyrrole conjugated compounds under spectroscopic, chromatographic and calorimetric investigation

Guido Angelini [a,*], Fabio Mantellini [b], Gianfranco Favi [b], Giacomo Mari [b], Carla Gasbarri [a,*]

[a] Department of Pharmacy, University "G. d'Annunzio" of Chieti-Pescara, via dei Vestini, Chieti, 66100, Italy
[b] Department of Biomolecular Sciences, Section of Chemistry and Pharmaceutical Technologies, University of Urbino "Carlo Bo", via Ca' Le Suore 2, Urbino, (PU), 61029, Italy

ARTICLE INFO

Keywords:
Curcumin-pyrrole
E-Z photoisomerism
Inclusion complex
SBE-βCD
Log k_w
ITC
HPLC
NMR

ABSTRACT

New synthesized curcumin-pyrrole derivatives, CurPy1, CurPy2 and CurPy3, were exposed to visible and UV light in solution at 298 K. In both cases remarkable spectral changes were generated according to irreversible *E-Z* photoisomerization involving one of the two double bonds in the curcuminoid unit. Photochemical degradation may also occurs depending on the irradiation time as confirmed by HPLC measurements. The lipophilic nature of each CurPy was quantified by measuring the experimental Log k_w value and the effect of sulfobutylether-β-cyclodextrin (SBE-βCD) in aqueous solution was observed. The host/guest stoichiometry and the binding constant values of the SBE-βCD/CurPy inclusion complexes were spectroscopically determined. Furthermore, the thermodynamic parameters obtained by Isothermal Titration Calorimetry (ITC) highlight that complexation occurs through a spontaneous process.

1. Introduction

Curcumin is a natural polyphenol isolated from the rhizome of *Curcuma longa*, generally associated with the therapeutical properties of turmeric, such as anti-inflammatory, neuroprotective, cardiovascular, antidiabetic, antioxidant, hepatoprotective and antineoplastic activities, owing to its high concentration in comparison to the other curcuminoids [1–5]. The major limits to the clinical use of curcumin consist in low bioavailability and high sensitivity to light [6–8]. The first one depends on the lipophilic nature of the molecule as described by the Log P value and can be overcome by applying a series of strategies to improve curcumin absorption and permeability, generally forming supramolecular systems based on cyclodextrins, liposomes and nanoparticles [9–12]; the second one depends on the *E-Z* photoisomerization of the methoxy-phenols attached symmetrically through an α, β-unsaturated-diketone unit also responsible of diketo/keto–enol tautomerism in aqueous solution [13,14]. It was observed that prolonged exposure to sunlight or UV radiation induces chemical degradation of curcumin in solid state and in solution causing the cleavage of the chain link between the two aromatic side rings of the molecule and the formation of small phenolic compounds rich in carboxylate groups, such as ferulic acid, vanillin, feruloyl methane and bicyclopentandione. Furthermore, phenolic polymerization of the degradation products may also occur [15–17].

It is well-known that the antioxidant property of curcumin depends on the phenolic hydroxyl groups of the molecule, while the rapid metabolism *in vivo* is mainly due to the central β-diketone moiety [18]. Structure-activity relationship studies highlighted that the introduction of a heterocyclic ring to mask the β-diketone group improves both stability and biological properties [19,20] In particular, curcumin-based pyrrole conjugates demonstrated better antibacterial property against *Staphylococcus aureus* in comparison to unmodified curcumin [21].

Pyrrole is a heterocyclic aromatic compound identified as a fundamental unit for natural and bioactive molecules [22,23]. Currently, pyrrole-derivatives were widely employed in the treatment of neurodegenerative and cardiovascular diseases, and also as antidepressant, antitumor, antioxidant, hepatoprotective, antihypertensive, anti-inflammatory and antidiabetic agents. Furthermore, antimicrobial, antiviral and anti-fungal effects were observed [21,24–28]. Although their remarkable properties curcumin-based pyrrole conjugates were still marginally studied. To further overcome the well-known limitations of curcumin and its derivatives mainly regarding their poor aqueous

* Corresponding authors.
E-mail addresses: guido.angelini@unich.it (G. Angelini), carla.gasbarri@unich.it (C. Gasbarri).

https://doi.org/10.1016/j.molstruc.2026.147346
Received 28 April 2026; Received in revised form 30 June 2026; Accepted 12 August 2026
Available online 13 August 2026
0022-2860/© 2026 The Authors. Published by Elsevier B.V. This is an open access article under the CC BY-NC-ND license (http://creativecommons.org/licenses/by-nc-nd/4.0/).

solubility, the formation of an inclusion complex based on cyclodextrins was successfully proposed. Currently, SBE-βCD offers a large series of advantages in comparison to native β-CD and its most common analogues, including higher versatility, lower toxicity and enhanced guest stabilization [29]. The presence of six to seven negatively charged sulfobutyl ether groups per molecule extends both the hydrophilic surface and the hydrophobic cavity enhancing steric and electrostatic interactions for binding capacity in host-guest complexation in the case of oral, parenteral, ocular, nasal, and inhalational administration [30]. For these reasons SBE-βCD is considered one of the most versatile solubility enhancers for many hydrophobic compounds, including curcumin. Cutrignelli *et al.* demonstrated, for example, that SBE-βCD increases curcumin solubility in aqueous solution from 0.56 to 102.78 μg/mL at 25° C by forming the host-guest complex with a binding constant of 1455 M^{-1}. Furthermore, *in vitro* test on the human hepatic cancer cell line HepG-2 pointed out that inclusion also provides an improvement in the curcumin anticancer and antioxidant activities due to the enhanced solubility of the guest [31].

The aim of this work was to investigate the photochemical behavior of three new synthesized CurPy (Fig.1) in solution after exposure to visible and UV light by using UV-vis, H^1-NMR and HPLC measurements. Stock ethanolic solutions of CurPy1, CurPy2 and CurPy3 were prepared and diluted samples were irradiated at 254 and 435 nm. The photochemical properties were also determined in DMSO. The interactions of each CurPy and the sulfobutylether-β-cyclodextrin in the formation of inclusion complexes were estimated in aqueous solution by measuring the relative binding constants (K_b) according to the Benesi-Hildebran method. Finally, the thermodynamic parameters of the inclusion process were calorimetrically estimated.

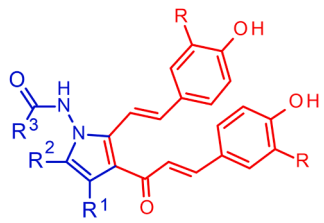
2. Materials

The NMR data and spectra of the bis-demethoxycurcumin-pyrroles derivates CurPy1 and CurPy3 and the curcumin-pyrroles derivates CurPy2 are available in Supplementary Material; sulfobutylether-β-cyclodextrin (SBE-βCD) was purchased by TCI Chemistry and used without further purification; Milli-Q water was used for the dilution of the samples. All solvents (ethanol, dimethyl sulfoxide, methanol 99% solvent spectroscopy grade) were purchased from Sigma-Aldrich.

2.1. Samples preparation for spectroscopic analysis

Stock ethanolic solution at a concentration of 2×10^{-3} M containing 10 % of dimethyl sulfoxide was obtained for each CurPy and kept in the dark at low temperature. The samples were prepared by diluting the stock solution to the final concentration of 2×10^{-5} M into a 1 cm light path quartz cuvette containing 2 mL of the proper solvent.

The stoichiometry and the binding constant (K_b) of the SBE-βCD/CurPy inclusion complex were determined according to Benesi



CurPy1: R=H, R^1=$CO_2(CH_2)_2OCH_3$, R^2= CH_3, R^3=NH_2

CurPy2: R=OCH_3, R^1=CO_2Et, R^2= CH_3, R^3=NH_2

CurPy3: R=H, R^1=CO_2Bn, R^2= CH_3, R^3=NH_2

Fig. 1. Structures of the investigated curcumin-pyrroles conjugates: CurPy1, CurPy2 and CurPy3.

Hildebran method described by Eqs. (1) and (2) as follows:

$$(A - A_0) = K_b\ \Delta\varepsilon\ [CurPy]\ [SBE-\beta CD]\ /\ (1\ + K_b\ [SBE-\beta CD]) \quad (1)$$

$$[SBE-\beta CD]\ [CurPy]\ /\ (A_0 - A)\ =\ 1/(K_b\ \Delta\varepsilon)\ +\ [SBE-\beta CD]\ /\ \Delta\varepsilon \quad (2)$$

where A and A_0 are the absorbance intensity of CurPy in the presence and in the absence of SBE-βCD, respectively; Δε is the difference in the molar absorption coefficients for free and complexed CurPy; K_b is the binding constant; [CurPy] and [SBE-βCD] are the total concentration of guest and host, respectively.

2.2. Photochemistry

The samples were irradiated at different exposure time, from 5 min up to 1 h, by using a Hg arc lamp (200W) equipped with a band pass interference filter centered at 435.0 and 254 +2 / -0 nm wavelength and 10.0 + 2 / 2 nm band width The UV–vis spectra of each sample were recorded at 25 °C by using a spectrophotometer Jasco V570.

2.3. ^{1}H-NMR analysis

CurPy1 was dissolved in $DMSO_{d6}$ at the concentration of 6×10^{-3} M. The sample was irradiated at 435 nm at 25 °C and the spectra were detected over time each 5 min for at least 1 h by using a Varian Mercury 300 MHz instrument equipped with VNMRJ 3.2 software.

2.4. HPLC analysis

ThermoFischer instrument equipped with TSP2000 pump, UV6000LP DAD detector and a chiral column R,R-DACH-DBN, 250×4.6 mm, 5 μm were used. A mixture of water and methanol as the eluent was prepared. The determination of the Log k_W was performed by using a percentage of MeOH in the range 30-55 % (v/v). The elution was carried out at 25° C with a flow of 0.7 mL/min. A plot of Log *k'* (where *k'* is the observed retention factor) against the methanol volume fraction φ in the mixture gives a straight line whose intercept corresponds to Log k_W.

The fraction of *E* isomer in the CurPy1, CurPy2 and CurPy3 solution was obtained by using 50/50 MeOH/ H_2O mixture as the eluent. The sample was injected after 15, 30, 45 and 60 min from irradiation at 435 nm.

2.5. ITC analysis

Calorimetric data were obtained by using the ITC 200 (Northampton, MA). An aliquot of the CurPy1 stock solution was diluted in ultrapure water and the appropriate amount of mixture ethanol/DMSO (90/10 v/v) was added to reach the 5% of organic solvent. An aliquot of the SBE-βCD 100 mM solution was diluted in ultrapure water containing the 5% of the mixture ethanol/DMSO (90/10 v/v). All samples were kept under vacuum for 5 min. Twenty injections were performed: the volume of the first injection consisted in 0.4 μL; the remaining 19 injections consisted in 2 μL. The reference cell and the sample cell of approximately 200 μL are both insulated by an adiabatic shield. The titration was carried out by stepwise injections of 10 mM SBE-βCD aqueous solution from a 40 μL injection syringe into the sample cell filled with 0.1 mM CurPy aqueous solution. The syringe is tailor-made such that the tip acts as a blade-type stirrer to ensure an optimum mixing efficiency at 1000 rpm. All measurements were carried out at a constant temperature of 25° C. Before performing the experiments the instrument was checked by water/water injection, noise control without injection and EDTA test. One set of site equation integrated in the Origin software of the instrument was used to process the calorimetric data. The 1:1 stoichiometry of CurPy/SBE-βCD was assumed as a constant parameter (fixed n=1 value) during the fitting because of our spectroscopical data come from the application of the Benesi-Hildebrand model.

3. Results and discussion

The UV-vis spectra of the CurPy1, CurPy2 and CurPy3 in ethanolic solution at 25 °C exhibit a maximum absorption band centered at 327 nm for CurPy1 and CurPy3 and at 335 nm for CurPy2 as reported in Fig. 2.

The absorbance of each CurPy is dependent on the concentration in the range 2×10^{-6} – 2×10^{-5} M according to the Lambert-Beer law (Fig. S1).

Interestingly, photoreactive behavior was observed by irradiation of the samples under visible and UV light. The spectral changes of the CurPy1 sample by exposure to 435 and 254 nm are reported in Fig. 3 as an example and suggest that *E-Z* isomerization of one of the two double bonds in the curcuminoid unit occurs according to the reaction previously observed in the case of ferulic acid and derivatives [32,33]. The UV-vis spectra of CurPy2 and CurPy3 are reported as Fig. S2 and S3, respectively.

H^1-NMR spectra of CurPy1 in $DMSO_{d6}$ solution show new peaks after irradiation. In the range 5.8-7.5 ppm the doublet of a *cis* double bond (5.97 ppm, J = 12.15 Hz), the doublet of the *trans* double bond (7.01 ppm, J = 15.84 Hz) and a new broad singlet due to -NH_2 of the *cis-trans* form can be observed [34] as highlighted by black arrows in Fig. 4.

The results suggest that the *E* and *Z* isomers co-exist in the investigated conditions and the reaction of photoisomerization occurs involving only one of the two double bonds in the curcuminoid unit of CurPy1 according to the cross peaks observed in the HH-COSY spectrum after irradiation (Fig. 5). The HSQC, HMBC and HH-COSY spectra of CurPy1 before irradiation are available in the Supplementary Material.

Interestingly, light exposition exceeding 15 min determines irreversible degradation of the molecule [35]. UV-vis spectra measurements confirm the photochemical behavior observed by NMR analysis. The spectral changes of 2×10^{-5} M CurPy1 in DMSO depending on the time of exposure at 435 nm were reported in Fig. 6.

The decreasing in the absorbance with the irradiation time and the presence of an isosbestic point up to 15 min of irradiation are due to the *E-Z* photoisomerization, while the gradual appearance of a weak intensity peak around 286 nm for irradiation time over 15 min can be considered as evidence of the photo-induced degradation of the sample as suggested by NMR analysis. Interestingly, the *E-Z* conversion induced by visible light observed in DMSO and ethanol solution occurs as irreversible reaction [34]. Similar photochemical behavior can be observed by exposure of the samples to UV light (Fig. S4).

In most cases the photoisomerism reaction is significantly fast and does not enable the separation of isomers [36]. HPLC measurements were performed to deeply study the photochemical properties of the investigated compounds. The appearance of an increasing peak after different irradiation time in the chromatograms of the samples clearly indicates the co-existence of the *E* and *Z* isomers. The chromatograms of CurPy1 in methanol/water mixture injected before and after 15, 30, 45 and 60 min of irradiation at 435 nm is shown as an example in Fig. 7.

The fraction of *E* isomer in solution was calculated as percentage of the non-irradiated sample using the peaks area before and after the light exposure. The data indicate that after 15 min of irradiation over 50% of the investigated CurPy maintain the *E* form according to a one-direction process, while from 30 to 60 min of irradiation no remarkable increase of the *Z* isomer peak can be observed, whereas the *E* isomer peak still decreases according to a photodegradation process. The percentage of *E* isomer at the different irradiation time, the Log k_w values for the investigated CurPy and calculated Log P are reported in Table 1.

Generally, the Log k_w value describes the lipophilic degree of the molecules allowing to estimate their affinity for the biological membranes. The Log k_w values of the investigated compounds were extrapolated from the linear correlation between the Log *k'* and the methanol volume fraction in the eluent mixture (Fig. S5). The trend in the Log k_w values for CurPy1, CurPy2 and CurP3 agrees with the Log P data as reported in Table 1. Interestingly, lower Log k_w of 3.22 and Log P of 2.70 were obtained in the case of the CurPy1 molecule suggesting moderate lipophilic nature in comparison to CurPy2 and CurPy3. Data from CurPy1 suggest an ideal hydrophobic/hydrophilic balance by which the molecule is generally able to cross cell membranes by passive diffusion, avoiding solubility problems or strong bound to plasma proteins [37, 38]. However, host-guest inclusion complex with SBE-βCD in aqueous solution were proposed herein to prevent self-aggregation and degradation of the investigated CurPy.

In the presence of SBE-βCD the maximum absorption band of the sample decreases and a slight bathochromic shift can be observed, furthermore no overlapping can be detected after irradiation at 435 nm for 15 min (Fig. 8). The spectral changes observed for CurPy1 in the SBE-βCD aqueous solution can be considered as evidence of the less polar microenvironment surrounding the guest molecules due to the insertion of CurPy1 into the hydrophobic cavity of the SBE-βCDs [39].

The photoconversion is inhibited in pure water but proceeds in the presence of SBE-βCD. Moreover, based on the absorbance values before and after irradiation, the guest undergoes a *E* to *Z* conversion of about 10% in the SBE-βCD aqueous solution. Since the depletion of the dominant isomer calculated after 15 min of irradiation strongly increased in ethanolic and DMSO solutions (Figs. 3 and 6), reaching 28.1% and 21.2%, respectively, the protective effect of cyclodextrin against the photoisomerization of the CurPy1 molecole can be clearly observed. The Benesi-Hildebrand plot of the difference between the absorbance of CurPy1 in aqueous solution the presence and in the absence of SBE-βCD versus the concentration of the sulfobuthylether-β-cyclodextrin is shown in Fig. 9. Data from CurPy2 and CurPy3 are reported as Fig. S6.

The host-guest stoichiometry of 1:1 inclusion complex was determined by the non-linear fitting [40]. The K_b value determined for the CurPy1, CurPy2 and CurPy3 is 1700, 470 and 1525 M^{-1}, respectively. Generally, inclusion complexes formed by using cyclodextrins as host show binding constants in the range 10–4000 M^{-1}. The relatively low K_b observed in the case of the SBE-βCD/CurPy complex suggests promising

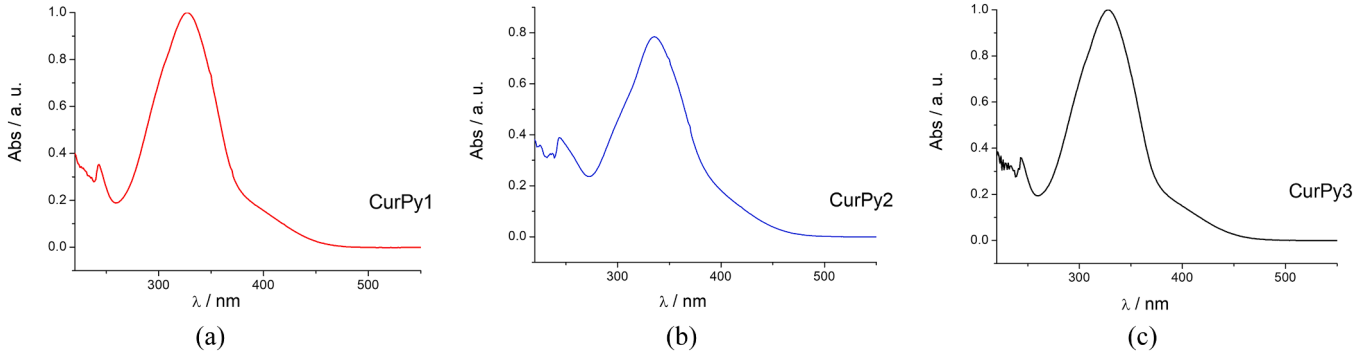


Fig. 2. UV-visible spectra of 2×10^{-5} M CurPy1 (**a**), CurPy2 (**b**) and CurPy3 (**c**) in solution at 25 °C.

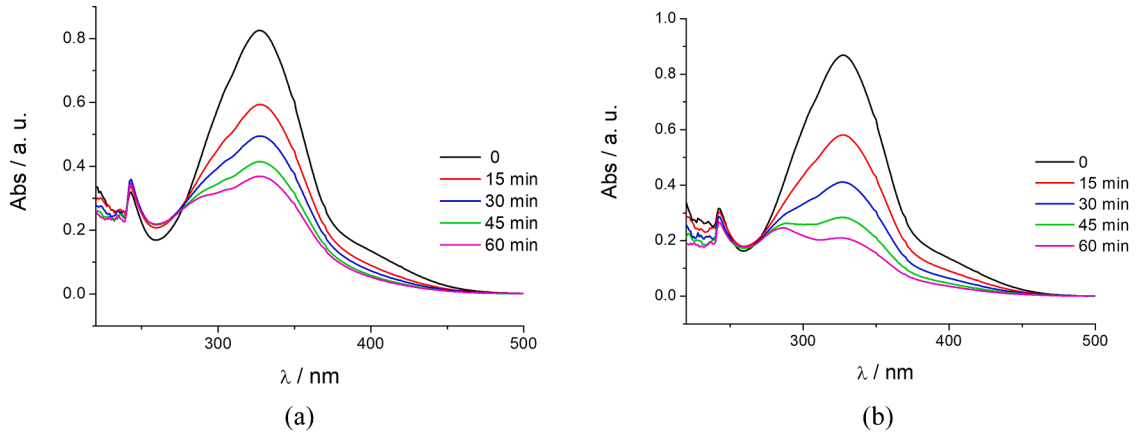


Fig. 3. UV-visible spectral changes of 2×10^{-5} M CurPy1 in ethanolic solution at 25 °C by irradiation at 435 nm (**a**) and 254 nm (**b**).

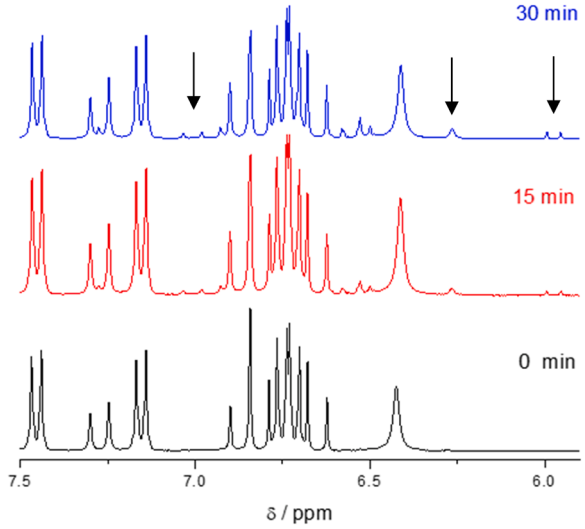


Fig. 4. ^{1}H-NMR spectra of CurPy1 in $DMSO_{d6}$ at different times of light exposure.

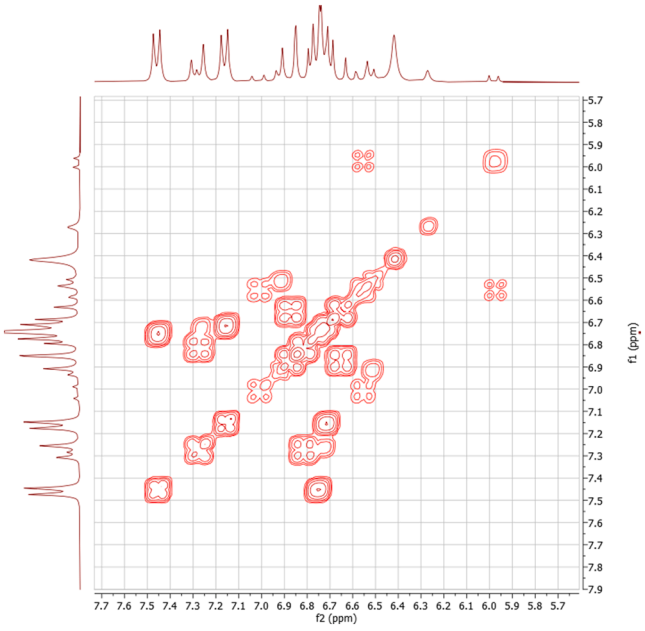


Fig. 5. HH-COSY spectrum of the CurPy1 molecule after irradiation for 30 min.

results in drug delivery by offering a prompt release of the guest from the cyclodextrin cavity [41]. Finally, ITC measurements provided the thermodynamic profile of the interactions involved between the investigated host and guest in aqueous solution at 25 °C as reported in Fig. 10.

The thermodynamic parameters of the investigated complexation were reported in Table 2.

The K_b of 1495 M^{-1} is comparable to the value spectroscopically obtained for CurPy1. Negative values of ΔH° and ΔS° were determined in the investigated conditions according to the typical enthalpic and entropic changes described for host-guest inclusion complexes formed by cyclodextrins [42–44]. Generally, negative ΔH° indicates that an exothermic process occurs according to a series of simultaneous effects involving the guest into the host cavity, mainly the generation of van der Waals forces, hydrogen bonds and electrostatic interactions, while negative ΔS° describes an endothermic process by which the translational and rotational degrees of freedom of the complexed guest are decreased in comparison to the free ones. In the case of the SBE-βCD /CurPy1 inclusion complex, the interactions between the guest and the host are enthalpically driven (ΔH° = -25.9 kJ/mol) and entropy opposed (ΔS° = -26.3 J/mol·K). Furthermore, the calculated Gibbs free energy (ΔG°= -18.1 kJ/mol) suggests that the formation of the SBE-βCD/-CurPy1 complex occurs according to a spontaneous process [45]. It was previously observed that the decreasing of the hydrophobic interactions between the SBE-βCD and the guest may depend on the hydrated sulfonated groups of the host leading to the distortion of the cyclodextrin cone and the inhibition of the guest insertion into the cyclodextrin cavity [46]. Similar thermodynamic parameters were previously obtained in the case of the formation of the SBE-βCD/Cyclocurcumin inclusion complex according to a spontaneous reaction [39].

4. Conclusion

The investigated curcumin-pyrrole derivatives exhibit irreversible *E-Z* photoisomerism both under visible and UV light. Photodegradation of the molecules also occurs for long irradiation time over 15 min as demonstrated by spectroscopic and chromatographic measurements. Among the investigated compounds CurPy1 is characterized by the best hydrophobic/hydrophilic balance and offers promising results as guest in the formation of the SBE-βCD/CurPy1 inclusion complex according to the ITC analysis. To the best of our knowledge the results reported herein are unprecedented and could contribute to the development of CurPy-based molecules as bioactive compounds for a large series of applications.

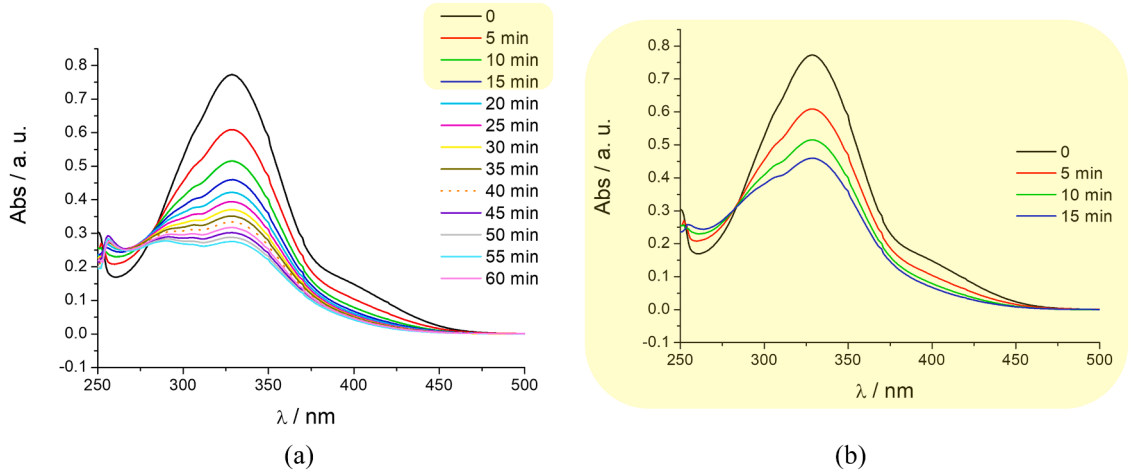


Fig. 6. UV-visible spectral changes of 2×10^{-5} M CurPy1 in dimethyl sulfoxide at 25 °C under irradiation to 435 nm. Each spectrum was determined after 5 min of exposition to light for at least 1 h (**a**), showing an isosbestic point up to 15 min (**b**).

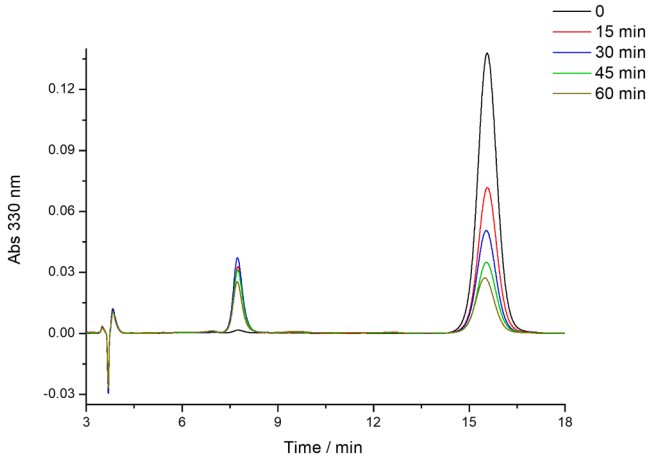


Fig. 7. Chromatograms of CURPy1 in methanol/water mixture injected after different irradiation time at 435 nm.

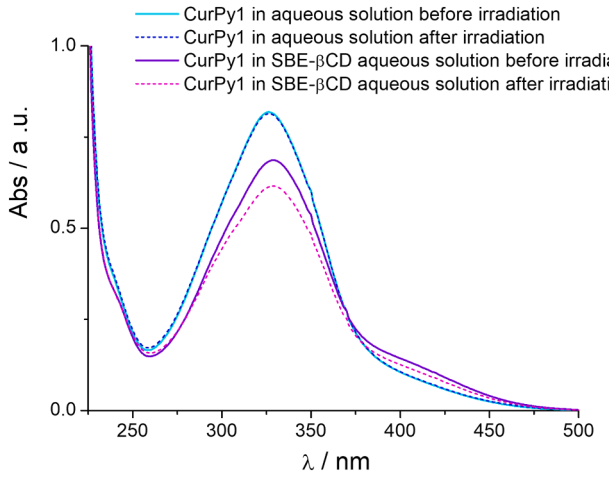


Fig. 8. Comparison between the UV-vis spectra of CurPy1 in aqueous solution at 25 °C in the presence and in the absence of SBE-βCD before and after irradiation at 435 nm for 15 min.

Table 1
Percentage of *E* isomer at the different irradiation time, Log k_w values and calculated Log P.

Sample	% *E* isomer in solution after different irradiation time				Log k_w	Log P [a]
	15 min	30 min	45 min	60 min		
CurPy1	58.0	39.0	29.9	21.2	3.22	2.70
CurPy2	59.2	30.7	22.3	15.6	3.68	2.92
CurPy3	59.1	31.7	24.7	19.6	4.17	4.15

[a] calculated by ADMET 3.0 software

Supporting information

Lambert-Beer plot of CurPy1, CurPy2 and CurPy3 in ethanolic solution; UV-vis spectra of CurPy2 and CurPy3 in ethanolic solution by irradiation at 435 and 254 nm; UV-vis spectra of CurPy1 in dimethyl sulfoxide by irradiation at 254 nm; determination of Log k_w for CurPy1, CurPy2 and CurPy3 and Benesi-Hildebrand plots of CurPy2 and CurPy3 in SBE-βCD aqueous solution at 25 °C; NMR spectra and data of CurPy1, CurPy2 and CurPy3 were available as Supplementary Material.

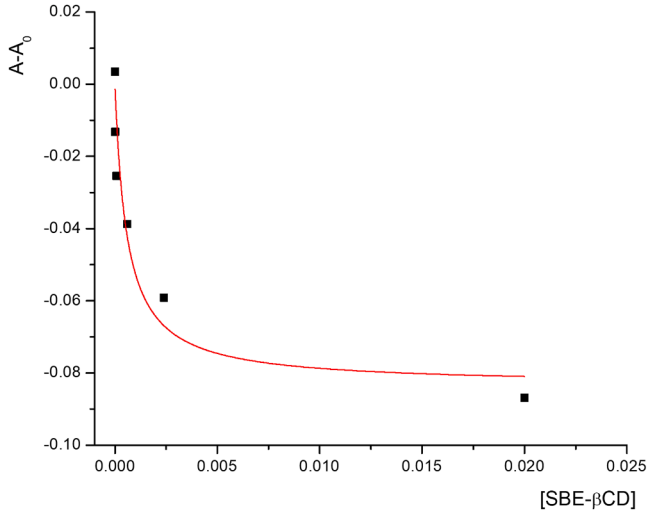


Fig. 9. Non-linear Benesi-Hildebrand plot for the SBE-βCD/CurPy1 inclusion complex.

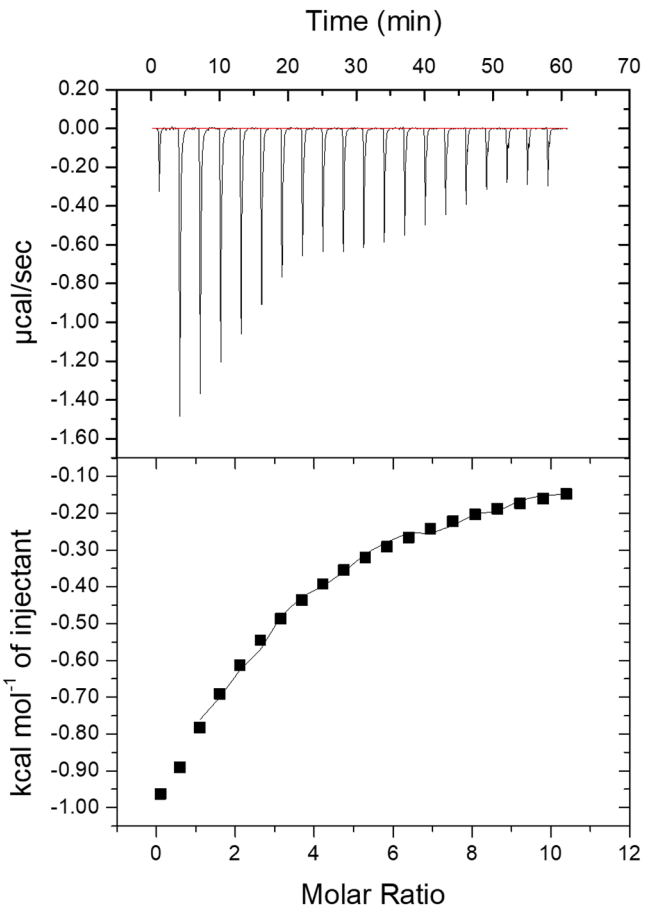


Fig. 10. Isothermal titration calorimetry profiles for CurPy1/SBE-βCD complex in aqueous solution at 25 °C. The upper panel represents the raw data for the titration of successive aliquots of SBE-βCD into CurPy1 solution. The bottom panel represents the integrated heat data after correction of the heat of dilution.

Table 2
Thermodynamic parameters of the CurPy1/SBE-βCD complexation. Each value is the mean of at least three independent experiments.

K_b (M^{-1})	ΔH° (kJ/mol)	ΔS° (J/mol·K)	ΔG° (kJ/mol)
1495 ± 85	-25.9 ± 4	-26.3 ± 13	-18.1 ± 0.1

CRediT authorship contribution statement

Guido Angelini: Data curation, Formal analysis, Investigation, Methodology, Writing – original draft, Writing – review & editing. **Fabio Mantellini:** Data curation, Resources, Writing – review & editing. **Gianfranco Favi:** Data curation, Resources, Writing – review & editing. **Giacomo Mari:** Data curation, Resources, Writing – review & editing. **Carla Gasbarri:** Conceptualization, Investigation, Project administration, Visualization, Writing – original draft, Writing – review & editing.

Declaration of competing interest

The authors declare that they have no known competing financial interests or personal relationships that could have appeared to influence the work reported in this paper.

Acknowledgments

This work was supported by University “G. d’Annunzio” of Chieti-Pescara.

Supplementary materials

Supplementary material associated with this article can be found, in the online version, at doi:10.1016/j.molstruc.2026.147346.

Data availability

Data will be made available on request.

References

[1] S.C. Gupta, S. Patchva, W. Koh, B.B. Aggarwal, Discovery of curcumin, a component of golden spice, and its miraculous biological activities, Clin. Exp. Pharmacol. Physiol. 39 (2012) 283–299, https://doi.org/10.1111/j.1440-1681.2011.05648.x.
[2] A.B. Kunnumakkara, M. Hegde, D. Parama, S. Girisa, A. Kumar, U.D. Daimary, P. Garodia, S.C. Yenisetti, O.V. Oommen, B.B. Aggarwal, Role of turmeric and curcumin in prevention and treatment of chronic diseases: lessons learned from clinical trials, ACS. Pharmacol. Transl. Sci. 6 (4) (2023) 447–518, https://doi.org/10.1021/acsptsci.2c00012.
[3] B.B. Aggarwal, B. Sung, Pharmacological basis for the role of curcumin in chronic diseases: an age-old spice with modern targets, Trends. Pharmacol. Sci. 30 (2009) 85–94, https://doi.org/10.1016/j.tips.2008.11.002.
[4] M.T. El-Saadony, A.M. Saad, D.M. Mohammed, S.S. Alkafaas, S. Ghosh, S.H. Negm, H.M. Salem, M.A. Fahmy, W.F.A. Mosa, E.H. Ibrahim, S.F. AbuQamar, K.A. El-Tarabily, Curcumin, an active component of turmeric: biological activities, nutritional aspects, immunological, bioavailability, and human health benefits - a comprehensive review, Front. Immun. 16 (2025), https://doi.org/10.3389/fimmu.2025.1603018.
[5] C. Gasbarri, G. Angelini, Cyclocurcumin as promising bioactive natural compound: an overview, Molecules 29 (2024) 1451, https://doi.org/10.3390/molecules29071451.
[6] S. Yan, X. Liao, Q. Xiao, Q. Huang, X. Huang, Photostabilities and anti-tumor effects of curcumin and curcumin-loaded polydopamine nanoparticles, RSC. Adv. 14 (2024) 13694–13702, https://doi.org/10.1039/d4ra01246a.
[7] G. Girst, S.B. Ötvös, F. Fülöp, G.T. Balogh, A. Hunyadi, Pharmacokinetics-driven evaluation of the antioxidant activity of curcuminoids and their major reduced metabolites-A medicinal chemistry approach, Molecules 26 (12) (2021) 3542, https://doi.org/10.3390/molecules26123542.
[8] C. Schneider, O.N. Gordon, R.L. Edwards, P.B. Luis, Degradation of curcumin: from mechanism to biological implications, J. Agric. Food Chem. 63 (35) (2015), https://doi.org/10.1021/acs.jafc.5b00244, 7606-14.
[9] S.B. de Souza Ferreira, M.L. Bruschi, Improving the bioavailability of curcumin: is micro/nanoencapsulation the key? Ther. Deliv. 10 (2) (2019) 83–86, https://doi.org/10.4155/tde-2018-0075.
[10] R. Tabanelli, S. Brogi, V. Calderone, Improving Curcumin bioavailability: current strategies and future perspectives, Pharmaceutics. 13 (2021) 1715, https://doi.org/10.3390/pharmaceutics13101715.
[11] L.Z. Racz, C.P. Racz, L.C. Pop, G. Tomoaia, A. Mocanu, I. Barbu, M. Sárközi, I. Roman, A. Avram, M. Tomoaia-Cotisel, V.A. Toma, Strategies for improving bioavailability, bioactivity, and physical-chemical behavior of Curcumin, Molecules. 27 (2022) 6854, https://doi.org/10.3390/molecules27206854.
[12] M. Hedge, S. Girisa, B. BharathwajChetty, R. Vishwa, A.B. Kunnumakkara, Curcumin formulations for better bioavailability: what we learned from clinical trials thus far? ACS. Omega 8 (2023) 10713–10746, https://doi.org/10.1021/acsomega.2c07326.
[13] G. Angelini, A. Pasc, C. Gasbarri, Curcumin in silver nanoparticles aqueous solution: kinetics of keto-enol tautomerism and effects on AgNPs, Colloids. Surf. Physicochem. Eng. Asp. 603 (2020) 125235, https://doi.org/10.1016/j.colsurfa.2020.125235.
[14] P. Cornago, R.M. Claramunt, L. Bouissane, I. Alkorta, J. Elguero, A study of the tautomerism of β-dicarbonyl compounds with special emphasis on curcuminoids, Tetrahedron. 64 (2008) 8089–8094, https://doi.org/10.1016/j.tet.2008.06.065.
[15] T. Tsuda, Curcumin as a functional food-derived factor: degradation products, metabolites, bioactivity, and future perspectives, Food Funct. 9 (2018) 705, https://doi.org/10.1039/c7fo01242j.
[16] K.I. Priyadarsini, Photophysics, photochemistry and photobiology of curcumin: studies from organic solutions, bio-mimetics and living cells, J. Photochem. Photobiol. C: Photochemistry 10 (2) (2009) 81–95, https://doi.org/10.1016/j.jphotochemrev.2009.05.001.
[17] M.V. Canamares, T.V. Garcia-Ramos, S. Sanchez-Cortes, Degradation of curcumin dye in aqueous solution and on Ag nanoparticles studied by ultraviolet–Visible absorption and surface-enhanced Raman spectroscopy, Appl. Spectrosc.. 2006, 60, 1386–1391, doi: 10.1366/000370206779321337.
[18] Y.M. Sun, H.Y. Zhang, D.Z. Chen, C.B. Liu, Theoretical elucidation on the antioxidant mechanism of curcumin: a DFT study, Org. Lett. 4 (2002) 2909–2911, https://doi.org/10.1021/ol0262789.
[19] Z. Liu, L. Tang, P. Zou, Y. Zhang, Z. Wang, Q. Fang, L. Jiang, G. Chen, Z. Xu, H. Zhang, G. Liang, Synthesis and biological evaluation of allylated and prenylated mono-carbonyl analogs of curcumin as anti-inflammatory agents, Eur. J. Med. Chem. 74 (2014) 671–682, https://doi.org/10.1016/j.ejmech.2013.10.061.
[20] S. Chakraborti, G. Dhar, V. Dwivedi, A. Das, A. Poddar, G. Chakraborti, G. Basu, P. Chakrabarti, A. Surolia, B. Bhattacharyya, Stable and potent analogues derived

from the modification of the dicarbonyl moiety of curcumin, Biochemistry 52 (2013) 7449–7460, https://doi.org/10.1021/bi400734e.
[21] N.G. Gogoi, A. Rahman, P. Dutta, J. Saikia, A. Baruah, J.G. Handique, Design, synthesis, biological evaluation and in Silico studies of Curcumin pyrrole conjugates, Chem. Biodivers. 21 (5) (2024) e202301605, https://doi.org/10.1002/cbdv.202301605.
[22] V. Bhardwaj, D. Gumber, V. Abbot, S. Dhiman, P. Sharma, Pyrrole: a resourceful small molecule in key medicinal hetero-aromatics, RSC. Adv. 5 (2015) 15233–15266, https://doi.org/10.1039/C4RA15710A.
[23] K. Seipp, L. Geske, T. Opatz, Marine Pyrrole Alkaloids, Mar. Drugs 19 (2021) 514, https://doi.org/10.3390/md19090514.
[24] T. Kundu, A. Pramanik, Expeditious and eco-friendly synthesis of new multifunctionalized pyrrole derivatives and evaluation of their antioxidant property, Bioorg. Chem. 98 (2020) 103734, https://doi.org/10.1016/j.bioorg.2020.103734.
[25] B. Sahu, R. Sahu, B. Gidwani, A. Mishra, Pyrrole: an essential framework in the development of therapeutic agents and insightful analysis of structure-active relationships, ChemistrySelect 9 (31) (2024) e202401604, https://doi.org/10.1002/slct.202401604.
[26] B.H. Ganesh, A.G. Raj, B. Aruchamy, P. Nanjan, C. Drago, P. Ramani, Pyrrole: A decisive scaffold for the development of therapeutic agents and structure-activity relationship, Chem. Med. Chem. 19 (2024) e202300447, https://doi.org/10.1002/cmdc.202300447.
[27] A. Rusu, O.L. Oancea, C. Tanase, L. Uncu, Unlocking the potential of pyrrole: recent advances in new pyrrole-containing compounds with antibacterial potential, Int. J. Mol. Sci. 25 (2024) 12873, https://doi.org/10.3390/ijms252312873.
[28] R.H. Abd El-Hameed, A.I. Sayed, S.Mahmoud Ali, M.A. Mosa, Z.M. Khoder, S. S. Fatahala, Synthesis of novel pyrroles and fused pyrroles as antifungal and antibacterial agents, J. Enzyme Inhib. Med. Chem. 36 (1) (2021) 2183–2198, https://doi.org/10.1080/14756366.2021.1984904.
[29] C.V. Pardeshi, R.V. Kothawade, A.R. Markad, S.R. Pardeshi, A.D. Kulkarni, P. J. Chaudhari, M.R. Longhi, N. Dhas, J.B. Naik, S.J. Surana, M.C. García, Sulfobutylether-β-cyclodextrin: a functional biopolymer for drug delivery applications, Carbohydr. Polym. 301 (2023) 120347, https://doi.org/10.1016/j.carbpol.2022.120347.
[30] A.A. Skuredina, I.M. Le-Deygen, E.V. Kudryashova, The effect of molecular architecture of sulfobutyl ether β-cyclodextrin nanoparticles on physicochemical properties of complexes with moxifloxacin, Colloid J. 80 (2018) 312–319, https://doi.org/10.1134/S1061933×18030134.
[31] A. Cutrignelli, A. Lopedota, N. Denora, R.M. Iacobazzi, E. Fanizza, V. Laquintana, M. Perrone, V. Maggi, M. Franco, A new complex of curcumin with sulfobutylether-β-cyclodextrin: characterization studies and in vitro evaluation of cytotoxic and antioxidant activity on HepG-2 cells, J. Pharm. Sci. 103 (12) (2014) 3932–3940, https://doi.org/10.1002/jps.24200.
[32] J.T. Hwang, Y. Kim, H.J. Jang, H.M. Oh, C.H. Lim, S. WoongLee, M.C. Rho, Study of the UV light conversion of feruloyl amides from Portulaca oleracea and their inhibitory effect on IL-6-induced STAT3 activation, Molecules 2016, 21, 865, doi:10.3390/molecules21070865.
[33] L. Moni, L. Banfi, A. Basso, A. Mori, F. Risso, R. Riva, C. Lambruschini, A thorough study on the photoisomerization of ferulic acid derivatives, Eur. J. Org. Chem. 11 (2021) 1737–1749, https://doi.org/10.1002/ejoc.202100064.
[34] M.A. Dettori, V. Ugone, D. Fabbri, P. Carta, A study on the photoisomerization of (E)-dehydrozingerone, its (E)-(E)-C2 symmetric dimer, and their O-methylated derivatives, Molecules 29 (2024) 5901, https://doi.org/10.3390/molecules29245901.
[35] G. Angelini, A. Gansmüller, J. Pécourneau, C. Gasbarri, An insight into cyclocurcumin cis–trans isomerization: kinetics in solution and in the presence of silver, J. Mol. Liq. 333 (2021) 116000, https://doi.org/10.1016/j.molliq.2021.116000.
[36] C. Dugave, L. Demange, Cis trans isomerization of organic molecules and biomolecules: implications and applications, Chem. Rev. 2003, 103, 2475–2532, doi: 10.1021/cr0104375.
[37] B. Testa, V. Pliska, H. van de Waterbeemd, Lipophylicity in Drug Action and Toxycology, 4, Wiley, New York, 1995, pp. 22–24, https://doi.org/10.1002/9783527614998.
[38] B. Testa, P.A. Carrupt, P. Gaillard, F. Billois, P. Weber, Lipophilicity in molecular modelling, Pharm. Res. 13 (3) (1996), https://doi.org/10.1023/a:1016024005429, 335-43.
[39] C. Gasbarri, G. Angelini, Combined calorimetric, spectroscopic, and microscopic investigation on the inclusion complex from cyclocurcumin and sulfobutylether-β-cyclodextrin, Colloids. Surf. Physicochem. Eng. Asp. 664 (2023) 131149, https://doi.org/10.1016/j.colsurfa.2023.131149.
[40] A.D. Bani-Yaseen, A. Moala, Spectral, thermal, and molecular modeling studies on the encapsulation of selected sulfonamide drugs in β-cyclodextrin nano-cavity, Spectrochim. Acta A: Mol. Biomol. Spectrosc. 131 (2014) 424, https://doi.org/10.1016/j.saa.2014.04.136.
[41] F. D'Aria, B. Pagano, C. Giancola, Thermodynamic properties of hydroxypropylβ-cyclodextrin/guest interaction: a survey of recent studies, J. Therm. Anal. Calorim. 147 (2022) 4889, https://doi.org/10.1007/s10973-021-10958-1.
[42] M.V. Rekharsky, Y. Inoue, Complexation thermodynamics of cyclodextrins, Chem. Rev. 98 (1998) 1875, https://doi.org/10.1021/cr970015o.
[43] K. Bouchemal, S. Mazzaferro, How to conduct and interpret ITC experiments accurately for cyclodextrin–guest interactions, Drug Discov. Today 17 (11-12) (2012), https://doi.org/10.1016/j.drudis.2012.01.023, 632-629.
[44] Y. Inoue, T. Hakushi, Y. Liu, L.H. Tong, B.J. Shen, D.S. Jin, Thermodynamics of molecular recognition by cyclodextrins. 1. Calorimetric titration of inclusion complexation of naphthalenesulfonates with α-, β-, and γ-cyclodextrins: enthalpy-entropy compensation, J. Am. Chem. Soc. 115 (1993) 475, https://doi.org/10.1021/ja00055a017.
[45] A. Basu, G.S. Kumar, Interaction of the dietary pigment curcumin with hemoglobin: energetics of the complexation, Food Funct. 5 (8) (2014) 1949, https://doi.org/10.1039/c4fo00295d.
[46] V. Zia, R.A. Rajewski, V.J Stella, Thermodynamics of binding of neutral molecules to sulfobutyl ether β-cyclodextrins (SBE-β-CDs): the effect of total degree of substitution, Pharm. Res. 17 (8) (2000) 936, https://doi.org/10.1023/a:1007571019908.